ELSEVIER

Preparation, characterization and biological activity of Fe(III), Fe(II), Co(II), Ni(II), Cu(II), Zn(II), Cd(II) and UO$_2$(II) complexes of new cyclodiphosph(V)azane of sulfaguanidine

Carmen M. Sharaby

Chemistry Department, Faculty of Science, Al-Azhar University (Girls), Nasr City, Cairo, Egypt

Abstract

Novel hexachlorocyclodiphosph(V)azane of sulfaguanidine, H$_4$L, l,3-[N'-amidino-sulfanilamide]-2,2,2,4,4,4-hexachlorocyclodiphosph(V)azane was prepared and its coordination behaviour towards the transition metal ions Fe(III), Fe(II), Co(II), Ni(II), Cu(II), Zn(II), Cd(II) and UO$_2$(II) was studied. The structures of the isolated products are proposed based on elemental analyses, IR, UV–vis, ^{1}H NMR, mass spectra, reflectance, magnetic susceptibility measurements and thermogravimetric analysis (TGA). The hyperfine interactions in the isolated complex compounds were studied using 14.4 keV γ-ray from radioactive ^{57}Co (Mössbauer spectroscopy). The data show that the ligand are coordinated to the metal ions via the sulfonamide O and deprotonated NH atoms in an octahedral manner. The H$_4$L ligand forms complexes of the general formulae [(MX$_z$)$_2$(H$_2$L)H$_2$O)$_n$] and [(FeSO$_4$)$_2$ (H$_4$L) (H$_2$O)$_4$], where X = NO$_3$ in case of UO$_2$(II) and Cl in case of Fe(III), Co(II), Ni(II), Cu(II), Zn(II) and Cd(II). The molar conductance data show that the complexes are non-electrolytes. The thermal behaviour of the complexes was studied and different thermodynamic parameters were calculated using Coats–Redfern method. Most of the prepared complexes showed high bactericidal activity and some of the complexes show more activity compared with the ligand and standards.

© 2005 Elsevier B.V. All rights reserved.

Keywords: Sulfaguanidine; Phosphorus pentachloride; Transition metal ions

1. Introduction

In recent years, structural feature of four-membered N$_2$P$_2$ ring compounds, in which the coordination number of P varies from three to five, has attached considerable attention [1]. Heterocycles with P–C, P–N, P–O and P–S bonds, in addition to their great biochemical and commercial importance [2], play a major role in some substitution mechanisms as intermediates or as transition states [2,3]. Also, some P containing heterocycles have been found to be potentially carcinostatics [2,3] among other pharmacological activities. The introduction of tervalent P centers in the ring enhances the versatility of the heterocycles in complexing with both hard and soft metals. Since the tervalent P centers can stabilize transition metals in low oxidation states, such complexes can be potential homogeneous or phase-transfer catalysts in various organic transformations.

There is considerable current interest in compounds containing spiro and ansaorganic P rings [4]. Although the ammonolysis of some 1,3-diaryl-2,4-dichlorocyclodiphosph-(V)azanes have been investigated in some detail [4], a little is known about the interaction of hexachlorocyclodiphosph(V)azanes with bifunctional reagents [4]. The reaction of bifunctional reagents with cyclodiphosph(V)azanes can give rise in principle to four types of structures: (i) spiro (both functional groups of reagent attached to the same P atom); (ii) ansa (the two functional groups attached to different P atoms in the same molecule); (iii) cross-linking (each functional group attached to different cyclodiphosph(V)azanes rings) to give small oligomeric units or polymers; (iv) only one functionality attached, whilst the other remains free. Spiro, ansa and cross-linking structures

---

E-mail address: csharaby@hotmail.com.

of phosphazanes are now well-studied synthetically, spectroscopically and crystallographically [4].

The reaction of hexachlorocyclodiphosph(V)azanes with amino compounds, active methylene containing compounds and bifunctional reagents have been investigated in some details [5,6]. Little is known about the interaction of hexachlorocyclodiphosph(V)azanes with therapeutic sulphonamides [5,6].

Sulfonamides are the oldest class of antimicrobials and are still the drug of choice for many diseases such as cancer and tuberculosis [7,8]. Cyclophosphamide and its derivatives are examples of phosphorus compounds, which are one of the most effective anticancer agents with proven activity against a large variety of human cancers [9]. Also, cyclodiphosph(V)azane-sulfonamide derivatives and their complexes have been prepared and the obtained compounds showed remarkable antimicrobial activity against various species of Gram-positive and Gram-negative bacteria [5,10]. An attempt to prepare hexachlorocyclodiphosph(V)azane of sulfonamides has been made using hexachlorocyclodiphosph(V)azane of sulfamethoxazole [11,12]. In this work, novel hexachlorocyclodiphosph(V)azanes of sulfaguanidine, H_4L, were prepared and the behaviour of this ligand towards some transition metal ions were studied using different techniques. Also, the bactericidal activity of these complexes was studied.

2. Experimental

2.1. Reagents

All chemicals used in this investigation were of analar grade, provided by B.D.H. chemicals. These include $FeCl_3 \cdot 6H_2O$, $FeSO_4 \cdot 7H_2O$, $CoCl_2 \cdot 6H_2O$, $NiCl_2 \cdot 6H_2O$, $CuCl_2 \cdot 2H_2O$, $ZnCl_2$, $CdCl_2 \cdot H_2O$ and $UO_2(NO_3)_2 \cdot 2H_2O$, sulfaguanidine and phosphorus pentachloride. The solvents used were dry ethanol, dry benzene, dry diethylether, dimethylformamide (DMF) and deutrated dimethyl sulfoxide (DMSO).

2.2. Synthesis of cyclodiphosph(V)azane of sulfaguanidine (H_4L)

The H_4L ligand was prepared using the methods of Chapmann et al. [13a], and Zhnurova and Kirsanov [13b]. Sulfaguanidine [N'-amidinosulsulfanilamide] (0.1 mol, 28.60 g) in 100 mL cold dry benzene, was added in small portions to a stirred cold solution (0.1 mol, 20.85 g) of phosphorus pentachloride in 100 mL cold dry benzene during half hour at $\simeq 15\,°C$. After the addition was completed, the reaction mixture was heated under reflux for 3 h under anhydrous conditions with continuous stirring (the experiment was done in a well-ventilated area because benzene is a cancer suspect agent). After the completion of the reaction

(HCl gas ceased to evolve), the reaction mixture was cooled to room temperature and the solids obtained were filtered, then washed several times with dry benzene and dry diethyl ether to give crystalline 1,3-di-[N'-(amidinosulfanilamide]-2,2,2,4,4,4-hexachlorocyclodipho-sph(V)azane.

2.3. Synthesis of complexes

A solution of the metal salts (10 mmol) in 50 mL dry ethanol was added dropwise to a solution of cyclodiphosph(V)azane of sulfa drug (5 mmol) in 100 mL absolute ethanol in a 2:1 metal to ligand molar ratio at room temperature with continuous stirring. After complete addition of the metal salt solution, the reaction mixture was heated under reflux for about 2 h under dry conditions. The complexes obtained were washed with dry ethanol then with dry diethyl ether and dried in vacuo. The products obtained give elemental analyses consistent with the proposed structures.

2.4. Instrumentation

The microanalyses of carbon, hydrogen, nitrogen and sulphur were carried out at the Microanalytical Center at Cairo University. The IR spectra were recorded on a Shimadzu FT-IR spectrometer using KBr discs. ^{1}H NMR spectra (DMSO-d_6) were recorded at room temperature, using TMS as internal standard. The solid reflectance spectra were measured using a Shimadzu PC 3101 spectrophotometer. Magnetic susceptibilities of the complexes in the solid state were recorded at room temperature on a Sherwood Scientific Magnetic Susceptibility Balance using the Faraday method. The molar conductance measurements were carried out using a Sybron–Barnstead conductometer. The thermogravimetric analyses (TG) were carried out on a Shimadzu TGA-50 H thermal analyzer. TGA was carried out in a dynamic nitrogen atmosphere (20 mL min^{-1}) with a heating rate of $10\,°C\,min^{-1}$. The electronic spectra of solutions of the complexes in DMF (10^{-3}M) were recorded on a Perkin-Elmer Lambda–3B UV–vis spectraphotometer. The mass spectra were performed by a Shimadzu-Ge-MS-Qp 100 EX mass spectrometer using the direct inlet system. Mössbauer measurements were performed in the Physics Department, Faculty of Science, Al-Azhar University, at room temperature in a transmission geometry employing ^{57}Co as a radioactive source. The spectra were analyzed using a computer program based on Lorentzian distribution. The isomer shifts were expressed relative to a metallic iron absorber.

Metal contents were determined complexometrically by standard EDTA titration [14]. The phosphorus content was determined gravimetrically as phosphorammonium molybdate using the Voy method [15]. The biological activity experiments were carried out at the Microbiology Laboratory at Cairo University, Cairo, Egypt.
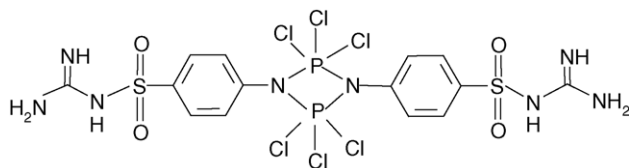
Fig. 1. Proposed structure of H_4L ligand.

3. Results and discussion

3.1. The ligand

The ligand in the present work, novel hexachloro-cyclodiphosph(V)azane of sulfaguanidine was prepared, using the methods of Chapmann et al. [13a], and Zhnurova and Kirsanov [13b]. Phosphorus pentachloride was reacted in cold dry benzene with sulfaguanidine to give 1, 3-di-[N'-amidinosulfanilamide]-2,2,2,4,4,4-hexachloro-cyclodiphosph(V)azane (H_4L) in 73% yield. The proposed structure for the ligand is shown in Fig. 1.

The assignment of the proposed structures for H_4L ligand is based on the correct elemental analyses for C, H, N, S and P (Table 1). The UV spectra of the ligand in DMF showed absorption band at 267 nm, which is characteristic for phosphazo four-membered ring of the dimeric structure [6,16]. The infrared spectra of the H_4L ligand showed the characteristic bands for *para*-disubstituted benzene rings. The ν(P–N), ν(SO_2), ν(C=N), ν(P–Cl) and ν(NH) values are summarized in Table 2. The ^{1}H NMR spectra of the ligand showed characteristic proton signals, which are listed in Table 3. Broad signals appeared at δ = 7.16, 7.37 and 5.82 ppm are characteristic of –SO_2NH, –C=(NH) and NH_2 proton signals, respectively. Further insight concerning the structure of the ligand was obtained from their mass spectra. The mass spectrometric fragmentation pattern of H_4L ligand (Scheme 1) showed a base peak at m/z 313 (100), together with peaks at m/z 368 (98), 314(24), 213 (97) and m/z 222 (23) which confirm the proposed structure of H_4L ligand (Fig. 1).

3.2. Metal complexes

Following the successful preparation of the ligand, attention was directed towards the chemical behaviour of the ligand H_4L towards transition metal ions. The metal ions selected for this purpose were Fe(III), Fe(II), Co(II), Ni(II), Cu(II), Zn(II), Cd(II) and UO_2(II).

When a mixture of 1 mol of H_4L ligand in dry ethanol was reacted with 2 mol of the metal salts in dry ethanol, a change in colour was observed and the complex compounds precipitated. The products were purified by washing with dry ethanol, and gave elemental analyses compatible with the suggested formulae given in Table 1 according to the following general equation:

$$2MX_z + H_4L + nH_2O \rightarrow [(MX_z)_2(H_2L)(H_2O)_n] + HX$$

Table 1
Analytical and physical data of the ligand H_4L and its complexes

Compound	m.p. (°C)	Colour (% yield)	% Found (calcd.)						μ_{eff} (B.M.)	Λ_m (Ω^{-1} mo^{-1} cm^2)
			C	H	N	S	P	M		
H_4L, $C_{14}H_{16}Cl_6N_8O_4P_2S_2$	180 ± 2	White (73)	24.30 (24.05)	2.45 (2.31)	15.81 (16.03)	9.35 (9.17)	8.55 (8.86)	–	–	–
$[(FeCl_2)_2(H_2L)(H_2O)_4]$, $C_{14}H_{22}Cl_{10}Fe_2N_8O_8P_2S_2$	>300	Yellow (51)	16.57 (16.44)	2.33 (2.17)	10.43 (10.96)	6.63 (6.27)	6.42 (6.06)	10.63 (10.92)	4.99	17.20
$[(FeSO_4)_2(H_4L)(H_2O)_4]$, $C_{14}H_{24}Cl_6Fe_2N_8O_{16}P_2S_4$	>300	Yellow (56)	15.33 (15.64)	2.53 (2.25)	10.60 (10.42)	11.62 (11.93)	5.88 (5.76)	10.05 (10.39)	5.20	16.52
$[(CoCl_2)_2(H_2L)(H_2O)_6]$, $C_{14}H_{26}Cl_8Co_2N_8O_{10}P_2S_2$	>300	Blue (60)	17.23 (16.92)	2.68 (2.64)	11.69 (11.27)	6.73 (6.45)	6.45 (6.23)	11.95 (11.86)	4.90	10.40
$[(NiCl_2)_2(H_2L)(H_2O)_6]$, $C_{14}H_{26}Cl_8Ni_2N_8O_{10}P_2S_2$	>300	Green (63)	17.22 (16.93)	2.00 (2.64)	11.53 (11.28)	6.82 (6.46)	6.53 (6.24)	12.13 (11.82)	2.95	8.37
$[(CuCl_2)_2(H_2L)(H_2O)_6]$, $C_{14}H_{26}Cl_8Cu_2N_8O_{10}P_2S_2$	>300	Yellow (76)	16.38 (16.76)	2.52 (2.61)	11.38 (11.17)	6.78 (6.39)	6.49 (6.18)	12.50 (12.67)	1.85	12.10
$[(ZnCl_2)_2(H_2L)(H_2O)_6]$, $C_{14}H_{26}Cl_8N_8O_{10}P_2S_2Zn_2$	>300	White (63)	16.85 (16.70)	2.35 (2.60)	11.42 (11.13)	6.52 (6.37)	6.03 (6.15)	13.12 (12.99)	diam.	9.89
$[(CdCl_2)_2(H_2L)(H_2O)_6]$, $C_{14}H_{26}Cd_2Cl_8N_8O_{10}P_2S_2$	>300	White (65)	15.56 (15.27)	2.32 (2.38)	10.66 (10.18)	6.22 (5.83)	5.44 (5.63)	20.63 (20.42)	diam.	10.30
$[(UO_2)_2(H_2L)(NO_3)_2(H_2O)_2]$, $C_{14}H_{18}Cl_6N_{10}O_{16}P_2S_2U_2$	>300	Yellow (60)	11.53 (12.03)	1.65 (1.30)	9.72 (10.02)	4.87 (4.59)	4.06 (4.43)	–	diam.	11.20

Table 2
IR spectra (4000–400 cm^{-1}) of the ligand H$_4$L and its complexes

Compound	ν(NH)	ν(C=N) (aliphatic)	ν(SO$_2$) (asym)	ν(SO$_2$) (sym)	ν(P-N)	ν(P-Cl)	ν(H$_2$O) (coord.)	δ(H$_2$O) (coord.)	ν(M-O)	ν(M-N)
H$_4$L	3160 br	1610 m	1310 sh	1032 sh	1162 sh	456 s	–	–	–	–
[(FeCl$_2$)$_2$(H$_2$L)(H$_2$O)$_4$]	3220 br	1544 m	1350 s	1088 br	1168 m	610 m	3340 br	796 s	548 m	455 s
[(FeSO$_4$)$_2$(H$_4$L)(H$_2$O)$_4$]	3200 br	1590 s	1350 m	1046 br	1138 br	560 m	3364 br	832 sh	510 s	460 s
[(CoCl)$_2$(H$_2$L)(H$_2$O)$_6$]	3220 br	1542 s	1332 sh	1090 sh	1172 sh	608 m	3414 br	830 sh	552 sh	470 s
[(NiCl)$_2$(H$_2$L)(H$_2$O)$_6$]	3206 br	1538 sh	1360 s	1092 m	1192 m	548 m	3418 br	828 sh	510 s	440 w
[(CuCl)$_2$(H$_2$L)(H$_2$O)$_6$]	3200 br	1534 sh	1350 m	1090 m	1172 m	548 m	3430 br	828 sh	520 s	453 w
[(ZnCl)$_2$(H$_2$L)(H$_2$O)$_6$]	3226 br	1536 sh	1350 m	1090 m	1164 m	546 m	3444 br	828 sh	500 m	440 s
[(CdCl)$_2$(H$_2$L)(H$_2$O)$_6$]	3218 br	1594 s	1348 s	1036 m	1164 m	550 m	3434 br	832 sh	500 s	450 s
[(UO$_2$)$_2$(H$_2$L)(NO$_3$)$_2$(H$_2$O$_2$)]	3200 br	1536 sh	1384 sh	1090 s	1168 m	600 m	3342 br	828 sh	548 m	480 s

sh: Sharp, m: medium, s: small, w: weak, br: broad.

Table 3
^{1}H NMR spectra of the ligand H$_4$L and its Zn(II) and Cd(II) complexes

Compound	Chemical shift, δ (ppm)	Assignment
H$_4$L	7.63	d, 4H, ArH's, $J = 8.58$ Hz
	6.92	d, 4H, ArH's, $J = 8.68$ Hz
	5.82	br, 4H, –C=(NH)(NH$_2$)
	7.16	br, 2H, -SO$_2$NH
	7.37	s, 2H, –C=(NH)
	–	br, coordinated H$_2$O protons
[(ZnCl)$_2$(H$_2$L)(H$_2$O)$_6$]	7.47	d, 4H, ArH's, $J = 8.42$ Hz
	6.67	d, 4H, ArH's, $J = 8.48$ Hz
	4.2	br, 4H, –C=(NH)(NH$_2$)
	6.72	br, 2H, -SO$_2$NH
	–	s, 2H, –C=(NH)
	4.0	br, coordinated H$_2$O protons
[(CdCl)$_2$(H$_2$L)(H$_2$O)$_6$]	7.65	d, 4H, ArH's, $J = 8.62$ Hz
	6.93	d, 4H, ArH's, $J = 8.62$ Hz
	4.9	br, 4H, –C=(NH)(NH$_2$)
	7.08	br, 2H, -SO$_2$NH
	–	s, 2H, –C=(NH)
	4.7	br, coordinated H$_2$O protons

$$2FeSO_4 + H_4L + 4H_2O \rightarrow [(FeSO_4)_2(H_4L)(H_2O)_4]$$
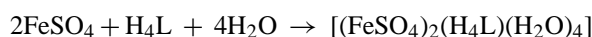
where M = Fe(III) (X = Cl, $z = 2$, $n = 4$); Co(II) (X = Cl, $z = 1$, $n = 6$); Ni(II) (X = Cl, $z = 1$, $n = 6$), Cu(II) (X = Cl, $z = 1$, $n = 6$); Zn(II) (X = Cl, $z = 1$, $n = 6$); Cd(II) (X = Cl, $z = 1$, $n = 6$) and UO$_2$(II) (X = NO$_3$, $z = 1$, $n = 2$).

The analytical data of the isolated complexes are listed in Table 1. Further, confirmation of the proposed structures of the chelates of the cyclodiphosph(V)azane of sulfa drug with metal salts was done using different physico-chemical methods shown below.

3.2.1. IR spectra and mode of bonding

The infrared spectra assignment of the proposed structures of the cyclodiphosph(V)azane of sulfa drug complexes was made through consideration of their infrared spectra. The coordinated stretching vibration bands of the isolated products were assigned by using a comparison method of infrared spectra comparing the spectra of the free ligand and its metal complexes.

The bands that appear near 3500–3400 cm^{-1} and 3400 cm^{-1} are due to ν_{asym}(NH$_2$) and ν_{sym}(NH$_2$) vibrations of the NH$_2$ group [17]. These vibration modes appear at higher or lower wavenumbers, compared with those of the free ligand. This may be due to that the hydrogen bonds involving the amino groups [17]. The bands at 1310 cm^{-1} and 1032 cm^{-1} are attributed to asymmetric and symmetric stretching vibrations, respectively, of the sulfone group, ν(O=S=O), in the free ligand. These bands are shifted to higher frequencies, at 1332–1384 cm^{-1} and 1036–1092 cm^{-1} upon coordination to the transition metals [12].

Also, the stretching vibration mode characteristic for ν(NH) of –C=(NH)(NH$_2$) moiety at 3160 cm^{-1} in the lig-
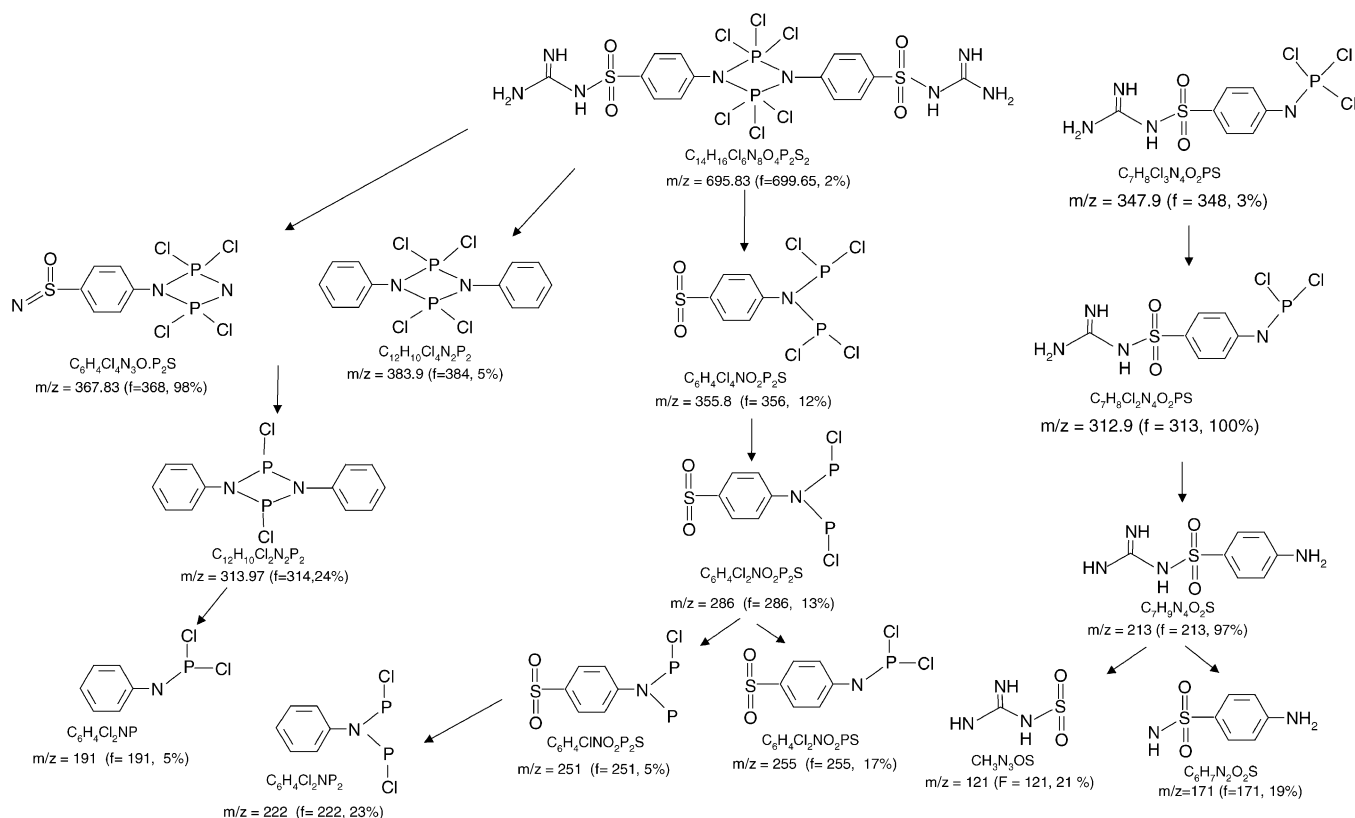
Scheme 1. Possible fragmentation pathways of H$_4$L ligand.

and was shifted to higher frequencies (3206–3220 cm^{-1}) in the complexes indicating the coordination via deprotonated NH group. This is also supported by the shift of the ν(C=N) stretching vibration band at 1610 cm^{-1} in the free ligand to 1590–1536 cm^{-1} in the complexes.

In all of the metal complexes, there are new medium to weak bands appearing at lower frequencies between 440–480 cm^{-1} and 500–552 cm^{-1}, which were assigned to ν(M–N) and ν(M–O) stretching modes, respectively [6,12,18,19]. These stretches were not present in the spectra of the ligand.

The appearance of bands at 3340–3444 cm^{-1} and 796–832 cm^{-1} is due to the stretching vibration and out of plane bending of coordinated water molecules in the spectra of the metal complexes.

3.2.2. Molar conductance data

The molar conductance data of the complexes ($\Lambda_m = 8.37$ to 17.20 Ω^{-1} mol^{-1} cm^2) in 10^{-3} M DMF solution at 25 °C, listed in Table 1, revealed that the complexes are non-electrolytes.

3.2.3. ^{1}H NMR spectra

The ^{1}H NMR spectra of the diamagnetic Zn(II) and Cd(II) complexes showed the same characteristic proton signals for the ligand. The signal characteristic for –C=(NH) group dis-

appeared in the spectra of the isolated complexes indicating coordination via deprotonated NH atom. Also, the signal characteristic for –NH$_2$ group shifted to lower frequencies due to the complexation.

3.2.4. Electronic spectra and magnetic properties

The UV–vis spectra of complexes in DMF solution showed absorption bands between 267 nm and 282 nm, which is characteristic of phosphazo four-membered rings [20,21]. However, the absorptions were red shifted with respect to the ligands depending on the types of metal ions present. The spectra of the Fe(III), Fe(II) and Cu(II) complexes further display a band in the range 365–440 nm, which might be assigned to charge transfer transition (most probably L → M CT) [22]. For the Co(II) complex, however, a d–d bands are observed at 600 nm and 675 nm which may attributed to the transitions $^4T_{1g}$ (F) → $^4T_{2g}$ (P) and $^4T_{1g}$ (F) → $^4A_{2g}$ (F), respectively, typical of octahedral structure around Co(II) ion [22].

The diffuse reflectance spectra of the complexes show bands at 249–250 nm, which are associated with interligand transitions.

From the diffuse reflectance spectrum of the Fe(III) complex, it is observed that a band at 22,421 cm^{-1} may be assigned to the $^6A_{1g} \rightarrow T_{2g}$ (G) transition in octahedral geometry [23]. Two bands, also, observed at 15,649 cm^{-1} and 17,482 cm^{-1} which can attribute to $^6A_{1g} \rightarrow {}^5T_{1g}$ transition.

The measured magnetic moment value of 5.99 B.M. confirm octahedral geometry involving sp^3d^2 hybridization in Fe(III) ion [24].

The diffuse reflectance spectrum of Fe(II) complex displays two absorption bands at 15,174 cm^{-1} and 22,222 cm^{-1} which are assigned to $^5T_{2g} \rightarrow {}^5E_g$ transitions [12,25]. Also, the band at 25,641 cm^{-1} is assigned to L $\rightarrow$ M charge transfer [25]. The observed magnetic moment of 4.90 B.M. is consistent with an octahedral geometry [25].

The electronic spectrum of the Co(II) complex displays two bands at 15,313 cm^{-1} and 17,482 cm^{-1} assigned to the $^4T_{1g} \rightarrow {}^4T_{1g}$ (P) and $^4T_{1g} \rightarrow {}^4T_{2g}$ (F) transitions, respectively, which arise due to ligand field transition of the pseudo octahedral component of the Co(II) complex. The observed magnetic moment value is $\mu_{eff} = 4.30$ B.M. at room temperature which confirms the octahedral structure of this cobalt complex [12]. The band observed at 22,624 cm^{-1} refers to L $\rightarrow$ M CT band.

The solid reflectance spectrum of the Ni(II) complex shows bands at 23,255, 17,482 and 18,917 cm^{-1}, suggesting the existence of $^3A_{2g} \rightarrow {}^3T_{1g}$ (P), $^3A_{2g} \rightarrow {}^3T_{1g}$ (F) and $^3A_{2g} \rightarrow {}^3T_{2g}$ transitions, respectively, with an octahedral spatial configuration. The observed magnetic moment of the complex is 2.95 B.M., which confirms the octahedral structure of this complex [12,26].

The solid reflectance spectrum of the Cu(II) complex gave a band at 16,806 cm^{-1}, which may be assigned to $^2E_g \rightarrow {}^2T_{2g}$ [27]. The observed magnetic moment of the Cu(II) complex is 1.85 B.M., which confirms the octahedral structure of this complex. The band observed at 22,935 cm^{-1} refers to L $\rightarrow$ M CT band.

The Zn(II), Cd(II) and UO$_2$(II) complexes are diamagnetic and in analogous to similar previously published data [12], they proposed to have octahedral structure.

3.2.5. Mössbauer measurements

The Mössbauer spectra were measured at room temperature for iron complexes. The spectra revealed the presence of Fe ions in [(FeCl$_2$)$_2$(H$_2$L)(H$_2$O)$_4$] and [FeSO$_4$)(H$_4$L)(H$_2$O)$_4$] in ferric and ferrous state respectively in octahedral coordination [28]. The Mössbauer parameters are listed in Table 5 and Fig. 2.

4. Thermal studies

Thermogravimetric studies (TGA) for the complexes were carried out within the temperature range from room temperature up to 1000 °C. The estimated mass losses were computed based on TG results and the calculated mass losses were computed using the results of microanalyses (Table 4). The determined temperature ranges and percent losses in mass of the solid complexes on heating are given in Table 4, which revealed the following findings.

The Fe(III) complex gives a decomposition pattern as follows: the first stage is two steps within the temperature range
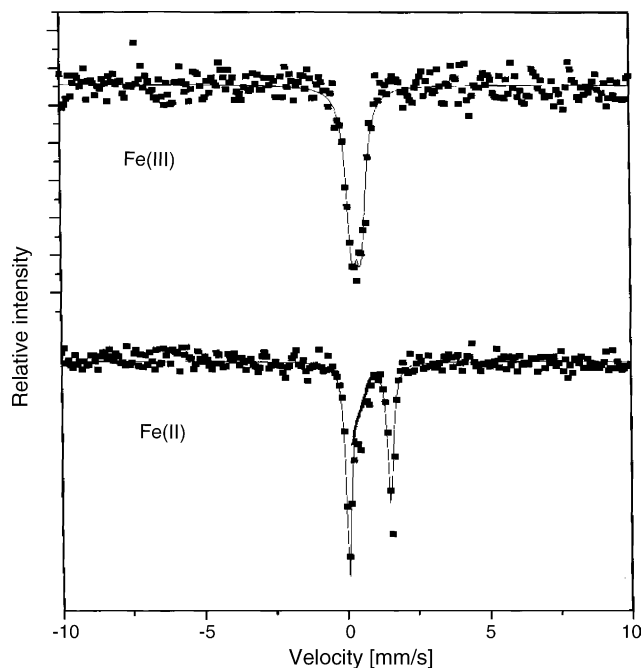

Fig. 2. Mössbauer spectra of the iron complexes.

of 40–250 °C, representing the loss of two coordinated water, 4HCl and O$_2$ gases with a found mass loss of 20.29% (calcd. 20.91%); the second stage is two steps within the temperature range 250–650 °C, represent the decomposition of the organic part with a found mass loss of 63.86% (calcd. 63.47%). At the end of the thermogram, the metal oxide, Fe$_2$O$_3$, was the residue 15.85% (calcd. 15.62%), which is in good agreement with the calculated metal content obtained and the results of elemental analyses (Table 1).

The thermogram of the Co(II) complex shows that the first and second weight losses are between 50 °C and 220 °C which represent the loss of five coordinated water molecules and 2HCl and 1/2O$_2$ gases with a found mass loss of 18.65% (calcd. 18.01%). The energy of activation (Table 5) is amounted to 44.53 kJ mol^{-1} and 89.48 kJ mol^{-1} for the first and second steps, respectively. The third, fourth and fifth steps: within the temperature range 220–950 °C, represent the decomposition of the organic part with a found mass loss of 65.80% (calcd. 65.30%) leaving behind Co$_2$O$_3$ as the product of decomposition. The energy of activation of the third, fourth and fifth steps respectively is amounted to 146.1, 115.2 and 92.31 kJ mol^{-1}.

The Ni(II) complex shows four steps of decomposition within the temperature range 40–750 °C. The first weight loss within the temperature range 40–210 °C represents the loss

Table 4

Mössbauer parameters for iron complexes of the H$_4$L ligand

Complex compound	Isomer shift (IS) (mm/s)	Quadrupole splitting (QS) (mm/s)
[(FeCl$_2$)$_2$(H$_2$L)(H$_2$O)$_4$]	0.42	0.72
[FeSO$_4$)$_2$(H$_4$L)(H$_2$O$_4$)]	1.6	3.6

Table 5
Thermogravimetric data of the ligand H_4L metal complexes

Complex	TG range (°C)	DTG_{max} (°C)	% Found (Calcd.)		Assignment	Metallic residue
			Mass loss	Total mass loss		
$[(FeCl_2)_2(H_2L)(H_2O)_4]$	40–250	70, 178	20.29 (20.91)		Loss of two coordinate H_2O, 4HCl and O_2	Fe_2O_3
	250–650	365, 520	63.86 (63.47)	84.15 (84.38)	Loss of $C_{14}H_{14}Cl_6N_8OP_2S_2$	
$[(CoCl_2)_2(H_2L)(H_2O)_6]$	50–220	89, 150	18.65 (18.01)		Loss of five coordinate H_2O, 2HCl, and $1/2O_2$	Co_2O_3
	220–950	270, 330, 730	65.80 (65.30)	84.45 (83.31)	Loss of $C_{14}H_{14}Cl_6N_8OP_2S_2$	
$[(NiCl_2)_2(H_2L)(H_2O)_6]$	40–210	87	17.89 (18.02)		Loss of five coordinate H_2O, 2HCl, and $1/2O_2$	2NiO
	210–750	360, 440, 580	66.45 (66.95)	84.34 (84.97)	Loss of $C_{14}H_{14}Cl_6N_8O_2P_2S_2$	
$[(UO_2)_2(H_2L)(NO_3)_2(H_2O)_2]$	130–260	211	6.99 (7.02)		Loss of two coordinate H_2O, NO_2 and $1/2O_2$	$2UO_2$
	260–800	310,361,635	55.00 (54.33)	61.99 (61.35)	Loss of NO_2, $1/2O_2$ and $C_{14}H_{14}Cl_6N_8O_4S_2P_2$	

of 2HCl, five coordinate water and $1/2O_2$ gases with a found mass loss of 17.89% (calcd. 18.02%). The activation energies of this step is amounted to 24.63 kJ mol^{-1}. The three remaining steps within the temperature range 210–750 °C may attributed to the decomposition of $C_{14}H_{14}Cl_6N_8O_2P_2S_2$ molecule with a found mass loss of 66.45% (calcd. 66.95%) leaving behind 2NiO as the product of decomposition. The activation energies of these steps are 67.69, 56.22 and 155.2 kJ mol^{-1} for the second, third and fourth steps, respectively.

The $UO_2(II)$ complex is thermally decomposed in four steps. The first step corresponds to a mass loss of 6.99% (calcd. 7.02%) within the temperature range 130–260 °C represents the loss of two coordinated water, NO_2 and $1/2O_2$ gases. The remaining steps; within the temperature range from 260–800 °C, with a found mass loss of 55.0% (calcd. 54.33%) is reasonably accounted for the decomposition of the organic part of the complex, $1/2O_2$ and NO_2 molecules leaving $2UO_2$ residue with a found mass loss of 38.01% (calcd. 38.65%).

M = Co(II), X = Cl
M = Ni(II), X = Cl
M = Cu(II), X = Cl
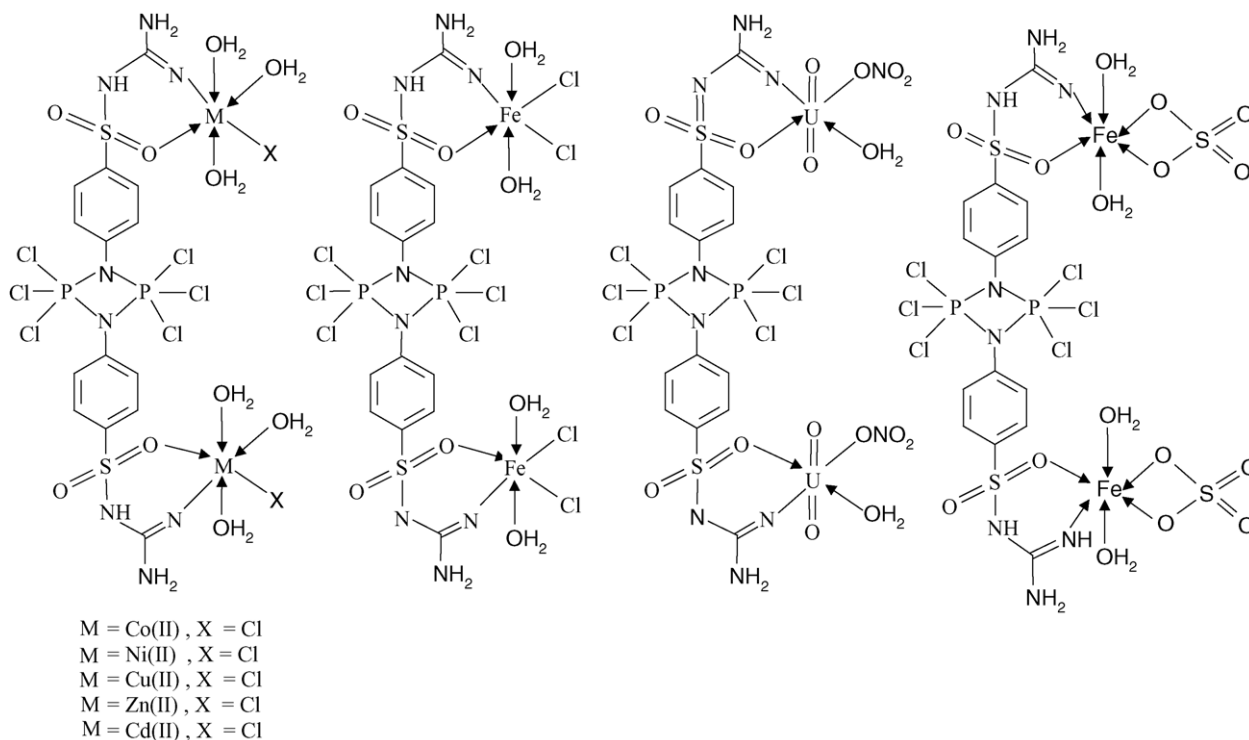M = Zn(II), X = Cl
M = Cd(II), X = Cl

Fig. 3. Suggested structural formulae of H_4L metal complexes.

Table 6
Thermodynamic data of the thermal decomposition of the complexes

Complex	TG range (°C)	E^* (kJ mol^{-1})	A (S^{-1})	ΔS^* (J K^{-1} mol^{-1})	ΔH^* (kJ mol^{-1})	ΔG^* (kJ mol^{-1})
[(FeCl$_2$)$_2$(H$_2$L)(H$_2$O)$_4$]	40–120	56.72	4.17×10^8	−33.15	35.25	55.02
	120–250	92.17	2.54×10^6	−72.82	66.75	76.22
	250–410	102.5	1.94×10^9	−105.3	53.63	66.35
	410–650	46.75	6.04×10^5	−68.75	106.3	96.53
[(CoCl$_2$)$_2$(H$_2$L)(H$_2$O)$_6$]	50–120	44.53	2.13×10^6	−33.05	68.15	54.73
	120–220	89.48	1.87×10^5	−63.06	79.75	59.13
	220–300	146.1	3.61×10^9	−97.83	112.5	112.4
	300–400	115.2	4.08×10^{10}	−66.35	105.6	84.58
	400–950	92.31	5.32×10^6	−76.49	53.64	126.3
[(NiCl$_2$)$_2$(H$_2$L)(H$_2$O)$_6$]	40–210	24.63	2.62×10^9	−29.23	56.32	68.16
	210–3900	67.69	3.09×10^7	−46.55	125.3	57.30
	390–500	56.22	6.53×10^9	−76.43	189.6	105.6
	500–750	155.2	4.83×10^{11}	−77.29	137.9	95.28
[(UO$_2$)$_2$(H$_2$L)(NO$_3$)$_2$(H$_2$O)$_2$]	130–260	33.65	3.05×10^7	−73.18	47.26	38.29
	260–330	60.28	4.58×10^{12}	−68.07	76.29	101.6
	330–400	117.3	1.99×10^7	−112.2	26.77	69.52
	400–800	72.80	3.52×10^{10}	−83.62	135.1	64.95

From the above thermogravimetric analyses, the overall weight losses for the Fe(III), Co(II), Ni(II) and UO$_2$(II) complexes agree well with the proposed formulae obtained by elemental analyses, IR, ^{1}H NMR, solid reflectance and magnetic susceptibility and Mössbauer measurements.

5. Kinetic studies

The kinetic parameters such as activation energy (E^*), enthalpy (ΔH^*), entropy (ΔS^*) and free energy change of the decomposition (ΔG^*) were evaluated graphically by employing the Coats–Redfern relation [29]:

$$\log \left[\frac{\log\{W_f/(W_f - W)\}}{T^2} \right]$$
$$= \log \left[\frac{AR}{\theta E^*} \left(1 - \frac{2RT}{E^*} \right) \right] - \frac{E^*}{2.303 RT} \quad (1)$$

where W_f is the mass loss at the completion of the reaction, W is the mass loss up to temperature T, R is the gas constant, E is the activation energy in kJ mol^{-1}, θ is the heating rate and $(1 - (2RT/E^*)) \cong 1$. A plot of the left-hand side of Eq. (1) against $1/T$ gives a slope from which E^* was calculated and A (Arrhenius constant) was determined from the intercept. The entropy of activation (ΔS^*), enthalpy of activation (ΔH^*) and the free energy change of activation ((ΔG^*) were calculated (Table 5). According to the kinetic data obtained from DTG curves, all the complexes have negative entropy, which indicates that activated complexes have more ordered systems than reactants.

6. Structural interpretation

From the above findings, we propose that the coordination occurs through the deprotonated nitrogen of the –C=NH(NH$_2$) moiety and the oxygen of the –SO$_2$NH group to give the following structures (Fig. 3).

Table 7
Antibacterial activity of H$_4$L and its metal complexes

Compound	Staphylococcus Pyogenes			Pseudomonas aeruginosa			Escherichia coli			Fungus(Candida)		
	5 mg/L	2.5 mg/L	1 mg/L	5 mg/L	2.5 mg/L	1 mg/L	5 mg/L	2.5 mg/L	1 mg/L	5 mg/L	2.5 mg/L	1 mg/L
H$_4$L	+++	++	+	++	+	−	++	++	+	−	−	−
[(FeCl$_2$)$_2$(H$_2$L)(H$_2$O)$_4$]	++	+	−	++	+	−	+	+	−	+	−	−
[(FeSO$_4$)$_2$(H$_4$L)(H$_2$O)$_4$]	++	++	+	++	+	−	++	++	+	+	+	−
[(CoCl$_2$)$_2$(H$_2$L)(H$_2$O)$_6$]	+++	++	++	++	+	+	+++	+++	++	+	−	−
[(NiCl$_2$)$_2$(H$_2$L)(H$_2$O)$_6$]	++	++	+	++	+	+	++	+	−	−	−	−
[(CuCl$_2$)$_2$(H$_2$L)(H$_2$O)$_6$]	+++	++	−	++	++	+	++	+	−	+	+	−
[(ZnCl$_2$)$_2$(H$_2$L)(H$_2$O)$_6$]	+++	++	++	+	+	++	++	+	+	+	−	−
[(CdCl$_2$)$_2$(H$_2$L)(H$_2$O)$_6$]	++	+	−	++	+	−	+	−	−	−	−	−
[(UO$_2$)$_2$(H$_2$L)(NO$_3$)$_2$(H$_2$O)$_2$]	++	+	+	++	++	+	++	+	+	+	−	−
Tavanic[a]	+++	++	+	+++	++	+	+++	++	+	−	−	−
Tarivid[a]	++	+	−	++	+	−	++	+	−	−	−	−

Inhibition values: 0.1–0.5 cm beyond control = +; inhibition values: 0.6–1.0 cm beyond control = ++; inhibition values: 1.1–1.5 cm beyond control = +++.
  [a] Standard materials.

7. Antimicrobial activity

Antifungal and antibacterial activities of the ligand H_4L and its metal complexes were studied against *Candida*, as a fungus *E. coli*, *Pseudomans aeruginosa* as gram-negative and *Staphylococcus pyogenes* as gram-positive bacteria at different concentrations of 1, 2.5 and 5 mg/mL in DMF as solvent by single disc method [30,31] using Tavanic and Tarivid as standard materials (Table 6).

From the antimicrobial results (Table 6), it is clear that the prepared ligand H_4L showed in some cases a higher activity than the tested standard. On the other hand, the prepared complexes in some cases demonstrated a significant higher antimicrobial activity than both the ligand and the standards (Table 7).

References

[1] S.S. Kumaravel, S.S. Krishnamurthy, J. Chem. Soc. Dalton Trans. 1 (1990) 1119–1121 (and references therein).
[2] M.S. Balakrishna, R. Panda, J.T. Mague, Inorg. Chem. 40 (2001) 5620–5625 (and references therein).
[3] (a) S. Priva, M.S. Balakrishna, J.T. Mague, S.M. Mobin, Inorg. Chem. 42 (2003) 1272–1281;
(b) M.S. Balakrishna, R.M. Abhyankar, J.T. Mague, J. Chem. Soc. Dalton Trans. (1999) 1407–1412.
[4] E. Ibrahim, I.M. Abd-Ellah, L.S. Shaw, I. Alnaim, J. Phosphorus Sulfur 33 (1987) 109–114 (and references therein).
[5] A.N. El-Khazandar, R.S. Farag, I.M. Abd-Ellah, Proc. Ind. Natl. Sci. Acad. Part A 60 (6) (1994) 793–801 (and references therein).
[6] I.M. Abd-Ellah, E.H.M. Ibrahim, A.N. El-Khazandar, J. Phosphorus Sulfur 31 (1987) 13–18 (and references therein).
[7] F.M. Arestrup, Int. J. Antimicrob. Agents 12 (1999) 279–285.
[8] E.X. Esposito, K. Baran, K. Kelly, J.D. Madura, J. Mol. Graph. Model. 18 (3) (2000) 283–289, and 307–308.
[9] K. Manabe, S. Kobayashi, Chem. Commun. (2000) 669–670.
[10] C. Sharaby, Al-Azhar Bull. Sci. 8 (1) (1997) 29–44.
[11] C. Sharaby, Ph.D. Thesis, Faculty of Science, Al-Azhar University (Girls), Cairo, Egypt 1992.
[12] C. Sharaby, Synth. React. Inorg. Met. Org. Chem., in press.
[13] (a) A.C. Chapmann, N.L. Paddock, H.T. Searle, J. Chem. Soc. (1961) 1825–1827;
(b) I.N. Zhnurova, A.V. Kirsanov, Zh. Obshch. Khim. 32 (1962) 2576–2580.
[14] G. Schwarzenbach, Complexometric Titrations, first ed., Interscience Publishers, London/New York, 1957, pp. 77–85.
[15] R. Voy, Chem. Ztg. Chem. Apparatus 21 (1897) 941.
[16] I.M. Abd-Ellah, E.H.M. Ibrahim, A.N. El-Khazandar, J. Phosphorous Sulfur 29 (1987) 239–248.
[17] A.G. Raso, J.J. Fiol, S. Rigo, A.L. Lopez, E. Molins, E. Espinosa, E. Borras, G. Alzuet, J. Borras, A. Castineiras, Polyhedron 19 (2000) 991–1004.
[18] M.A. El-Ries, S.M. Abu-El-Wafa, F.A. Aly, Egypt. J. Pharm. Sci. 26 (14) (1985) 1–7.
[19] J.R. Ferraro, Low Frequency Vibrations of Inorganic and Coordination Compounds, first ed., Plenum Press, New York, 1971, pp. 168–196.
[20] M.S. Masoud, Z.M. Zaki, Trans. Met. Chem. 13 (5) (1988) 321–327.
[21] G.G. Mohamed, Spectrochim. Acta Part A 57 (2001) 1643–1698.
[22] A.S.A. Zidan, A.I. El-Said, M.S. El-Meligy, A.A.M. Aly, O.F. Mohamed, J. Therm. Anal. 62 (2000) 665–679.
[23] M.M. Moustafa, J. Therm. Anal. 50 (1997) 463–771.
[24] G.G. Mohamed, N.E.A. El-Gamel, F.A. Nour El-Dien, Synth. React. Inorg. Met. Org. Chem. 31 (2) (2001) 347–358.
[25] F.A. Cotton, G. Wilkinson, C.A. Murillo, M. Bochmann, Advanced Inorganic Chemistry, sixth ed., Wiley, New York, 1999.
[26] A.B.P. Lever, Inorganic Electronic Spectroscopy, first ed., Elsevier Publishers, London/New York, 1968, pp. 267–355.
[27] Z.M. Zaki, Spectrosc. Lett. 31 (4) (1998) 757–766.
[28] N.N. Greenwood, T.C. Gibb, Mössbauer Spectroscopy, first ed., Champan and Hall Ltd. Publishers, London, 1971, pp. 248–251.
[29] A.W. Coats, J.P. Redfern, Nature 201 (1961) 68–69.
[30] J.D. Sleight, M.C. Timburg, Notes on Medical Bacteriology, second ed., Churchill Publishers, Livengstone, USA, 1981, p. 43.
[31] I.M. Abd-Ellah, M.E. Hussein, A.N. El-Khazandar, R.S. Farag, Oriental Chem. 7 (3) (1991) 121–127.